This poster participates in OSP

Outstanding Student Poster Contest

European Geosciences Union General Assembly 2016
Vienna, Austria, 17-22 April 2016
Session HS7.4: Change in climate, hydrology and society,
Vol. 18, EGU2016-15137.

Stochastic investigation of precipitation process for climatic variability identification

Alexia Sotiriadou, Amalia Petsiou, Elissavet Feloni, Paris Kastis, Theano Iliopoulou, Yannis Markonis, Hristos Tyralis, Panayiotis Dimitriadis and Demetris Koutsoyiannis

The poster can be downloaded at: http://www.itia.ntua.gr/

Department of Water Resources
and Environmental Engineering
National Technical University of Athens

1. Introduction

In the past few years, climate variability has been the subject of many scientific studies, strongly correlated with precipitation [1]. Most of these researches have reached the conclusion that precipitation is highly affected by climate variability. Throughout the Earth's history, this variability is regarded by some as an unusual phenomenon, that leads to the common belief that it may be caused by human intervention. This point of view entails significant difficulties to estimate statistical features in large time scales with acceptable reliability and increases the uncertainty of hydrological processes. Such problems are related to the fact that climatic models are necessarily simplified representations of the complex climate system since they do not describe completely the dynamics of all the involved processes [2].

The aforementioned studies do not usually take into consideration the full dynamics of the climate system. However, there are other dynamics such as Hurst-Kolmogorov [3] that are based on entropy maximization and therefore permit the estimation of wider range of statistical variability. The features describing this variability may vaguely change in time when the process exhibits Hurst-Kolmogorov behavior. Therefore this raises the question whether the observed change in a physical process induce hydrometerological persistence or anthropogenic activity. Here, we examine the climatic variability of precipitation based on observations from over 100000 stations with long (over 100 years) records from around the globe.

Aim: Is it possible to describe the climatic variability of mean annual precipitation by using only three parameters? These parameters are the mean, standard deviation and Hurst coefficient with the latter estimated through the climacogram (i.e., plot of variance or standard deviation of the mean-scaled random variable versus scale). The justification for the use of the climacogram as a measure of statistical uncertainty can be seen in [4]).

2. Methodology

The statistical uncertainty enclosed within the precipitation process is quantified through a Monte Carlo approach. The analysis is based on the assumptions that the ratio of the annual mean precipitation divided by the annual standard deviation is a stationary process, normally distributed and that it follows one of the most commonly used stochastic models in geophysics, i.e., Markov and HK (including the White Noise process for H=0.5). These assumptions are not only parsimonious but also considered conservative since any non-stationary approach would increase the complexity of the system, the probability function is likely it has a non-Gaussian tail and the stochastic structure cannot be any less complex that the Markov and HK one-parameter models, which entail all exponential as well as a power-type behaviours. Furthermore, the analysis is applied for all climatic zones described in the Koppen system. Moreover, each mean annual value is considered valid when it is estimated from more than 300 days, i.e. one measurement per day for at least 10 months. For the synthesis of the stochastic timeseries, we use the 3×AR(1) technique described in [2]:

The stationary process is produced as a sum of 3 stationary Markov processes, xi = Ai + Bi + Ci. The processes A, B, C have the following characteristics:

Autocorrelation coefficient for lag 1:

$$\rho_a = 1.52\ (H - 0.5)^{1.32}$$
$$\rho_b = 0.953 - 7.69\ (1 - H)^{3.85}$$
$$\rho_c = 0.932 + 0.087\ H, \text{ for } H < 0.76,$$
$$\rho_c = 0.993 + 0.007\ H, \text{ for } H > 0.76$$

Variance:

$$\sigma^2_a = (1 - c_1 - c_2)\ \gamma_0$$
$$\sigma^2_b = c_1\ \gamma_0$$
$$\sigma^2_c = c_2\ \gamma_0$$

Where γ_0: the variance of real time series and c_1 and c_2: calculated in a way that the correlation coefficient of the real time series be the same as the synthetic's for hysteresis 1 and 100.

Based on the Monte Carlo results, we estimate the prediction interval (prediction error) of each 30-year mean, standard deviation, minimum and maximum values. The prediction interval is actually a measurement ranging from zero to one that compares the 30-year values observed in each station with the ones predicted from the model. In this manner, we are able to capture any large, medium or low 30-year climatic variability that occurred in approximately the last 100 years.

3. Spatial Distribution of Stations

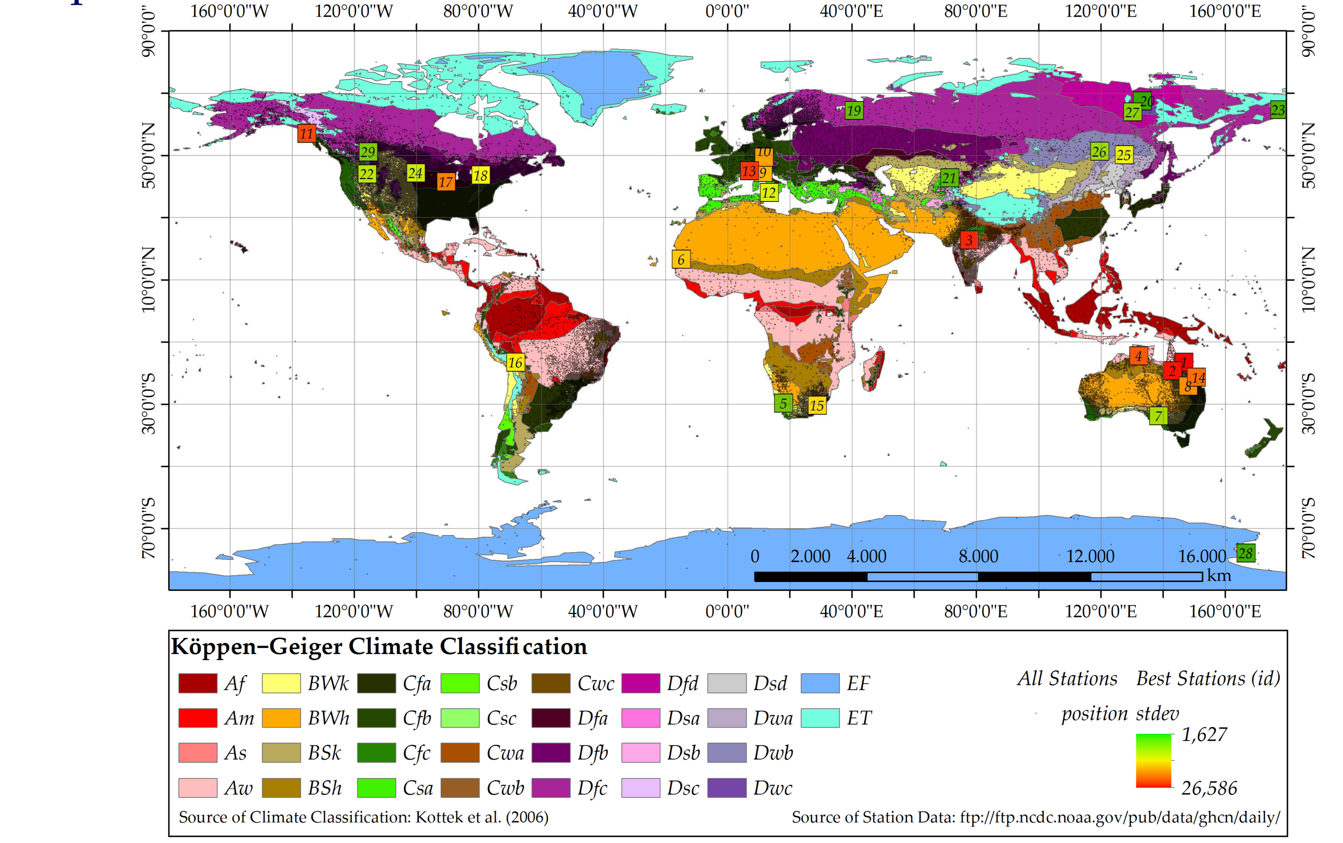

Map 1: Köppen Climate Classification, with the station network. A total of 100198 stations were selected [5].

4. Basic Features of High Credibility Stations

Station ID	N_0 (Prop Dry)	Mean (mm)	Stdev (mm)	Skewness	Kurtosis	$\hat{H}$	Height (m)	Köppen	Location
1	0.55	9.64	26.59	6.01	57.17	0.36	10	Af	Queensland, NE Australia
2	0.65	5.65	19.85	7.86	96.43	0.42	4	Am	Queensland, NE Australia
3	0.78	3.48	13.16	6.98	74.42	0.80	302	As	Hoshangabad, Madhya Pradesh, India
4	0.83	2.50	9.66	6.94	78.19	0.62	106	Aw	Northern Territory, Australia
5	0.90	0.64	3.34	10.75	188.67	0.76	1007	BWk	Springbok, Northern Cape, South Africa
6	0.90	1.09	5.79	8.89	113.68	0.72	7	BWh	Senegal, Western Africa
7	0.73	1.54	4.66	6.16	67.53	0.39	368	BSk	South Australia
8	0.84	1.78	7.57	7.89	93.50	0.41	344	BSh	Queensland, East Australia
9	0.74	1.84	5.98	6.13	60.05	0.81	53	Cfa	Bologna, North Italy, Europe
10	0.46	3.27	6.56	3.92	28.62	0.75	977	Cfb	Bavaria, Germany, Central Europe
11	0.31	7.12	11.36	3.28	20.33	0.63	20	Cfc	Alaska, NW North America
12	0.74	1.49	5.01	7.01	79.73	0.77	37	Csa	Sicily, Mediterranean Sea
13	0.69	3.49	11.76	7.59	112.70	0.52	55	Csb	NW Italy, Southern Europe
14	0.83	1.93	8.85	10.50	188.21	0.47	195	Cwa	Queensland, W.NW Australia
15	0.78	1.92	5.71	4.78	34.71	0.11	1490	Cwb	Matatiele, Eastern Cape, South Africa
16	0.60	2.20	5.70	8.61	147.98	1.00	4061	Cwc	La Paz, Bolivia, South America
17	0.71	2.50	8.07	6.24	62.59	0.56	173	Dfa	Iowa-Illinois Borders, USA
18	0.61	2.24	5.67	4.67	35.47	0.72	113	Dfb	Toronto, Eastern Canada
19	0.47	1.44	3.16	5.12	45.86	0.86	8	Dfc	Arkhangelsk, Russia, Europe
20	0.72	0.44	1.63	9.03	130.31	0.56	136	Dfd	Sakha Republic Russia, Northern Asia
21	0.79	0.82	3.06	8.36	137.83	0.75	655	Dsa	Taraz, Kazakhstan, Asia
22	0.74	1.67	4.67	4.75	37.82	0.56	944	Dsb	Idaho, USA
23	0.66	0.80	2.45	6.04	53.85	0.75	64	Dsc	Chukotka Autonomous Okrug, NE Russia, Asia
24	0.76	1.25	4.68	6.97	70.35	0.71	531	Dwa	South Dakota, USA
25	0.74	1.50	5.26	6.50	64.96	0.57	130	Dwb	Blagoveshchensk, Eastern Asia
26	0.77	1.10	4.28	7.39	80.85	0.69	621	Dwc	Zabaykalsky Krai Russia, Eastern Asia
27	0.66	1.10	3.59	6.81	73.82	0.19	208	Dwd	Sakha Republic Russia, Northern Asia
28	0.81	0.47	2.00	10.37	167.93	0.77	24	EF	Hut Point Peninsula, Antarctica
29	0.65	1.27	3.50	5.96	61.82	0.40	1384	ET	Banff, Alberta, Canada

Table 1: Best Stations - basic characteristics – daily precipitation

5. Q-Q plots

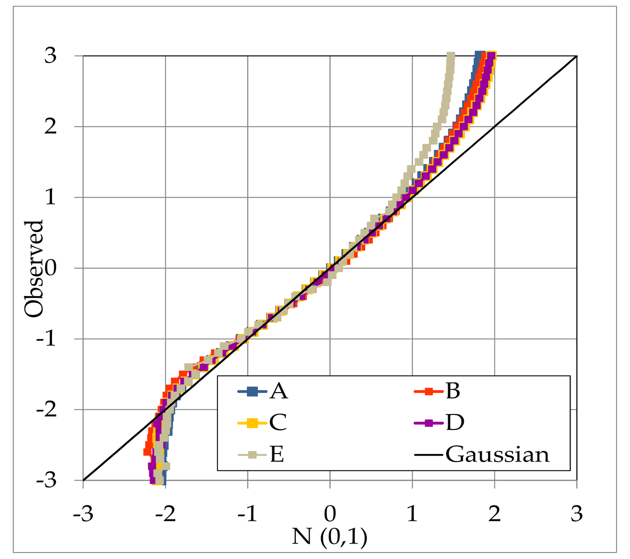

Figure 1: Q-Q plots of avg per climate type

Figure 1 illustrates the relationship between the distribution of the observed timeseries and the Gaussian distribution. It can be noticed that the distribution approximates normality, except for the extreme values of the upper limit which differ from the Gaussian distribution. This deviation does not occur to such extent at the low values due to the zero barrier of precipitation.

It can be observed in Figure 2 that between quartile 25% and 75% of the q-q values, data adequately approximate normality. For the 5% and 95%, there is a significant deviation from the Gaussian distribution. The latter observation is somehow expected due to the non-Gaussian heavy tail of precipitation.

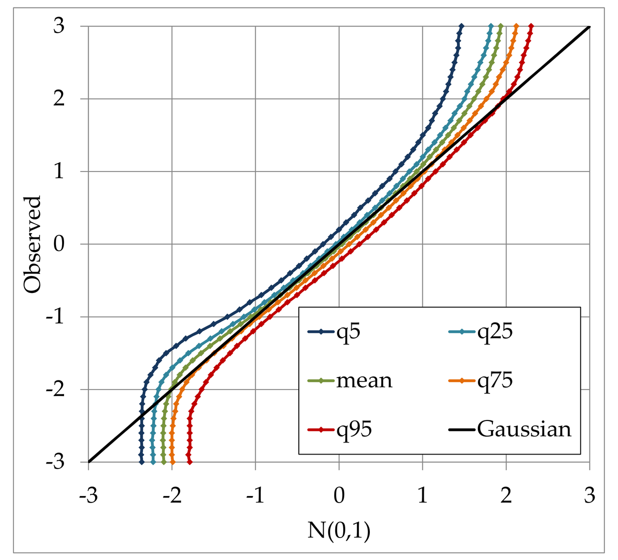

Figure 2: Q-Q plots of quartiles

6. Climacograms

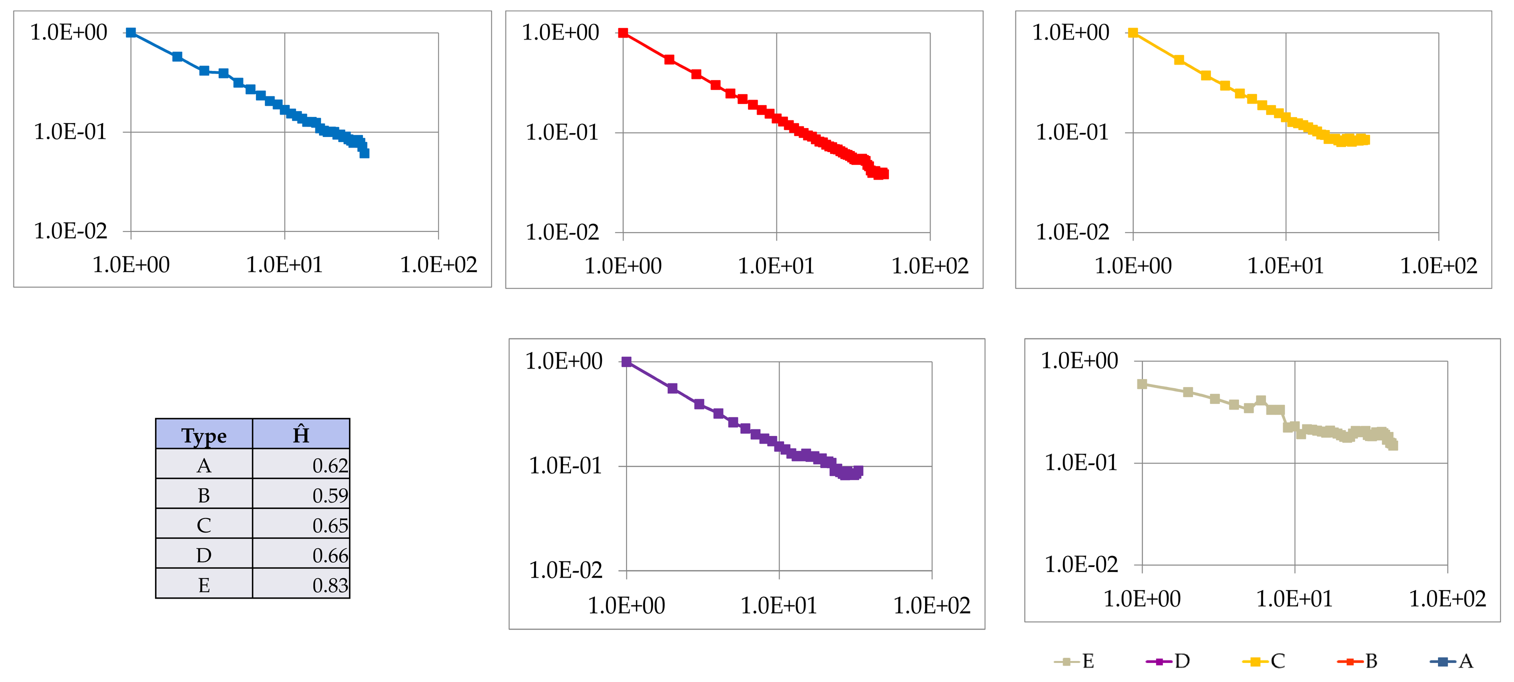

Type	$\hat{H}$
A	0.62
B	0.59
C	0.65
D	0.66
E	0.83

Figure 3: Climacograms observed (empirical averaged)

The resulted climacograms show no significant variation based on the Koppen categorization. An exception to the above observation is the Köppen E group (polar climate) where the Hurst coefficient is estimated around 0.85.

7. Mean vs. stdev of daily precipitation

The mean values are plotted versus standard deviation. This Figure actually shows the correlation between mean and stdev and from that we can induce that stdev increases as a power law with the mean. This is somehow reasonable because of the zero barrier of precipitation (dry days). Specifically, even in the most rainy areas of the tropic zones there may be dry days, so along with the mean value the value of the stdev is expected to increase too.

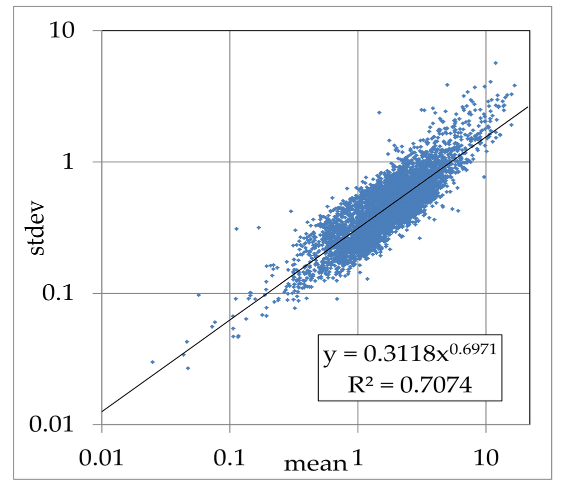

Figure 4: Best stations (mean, stdev)

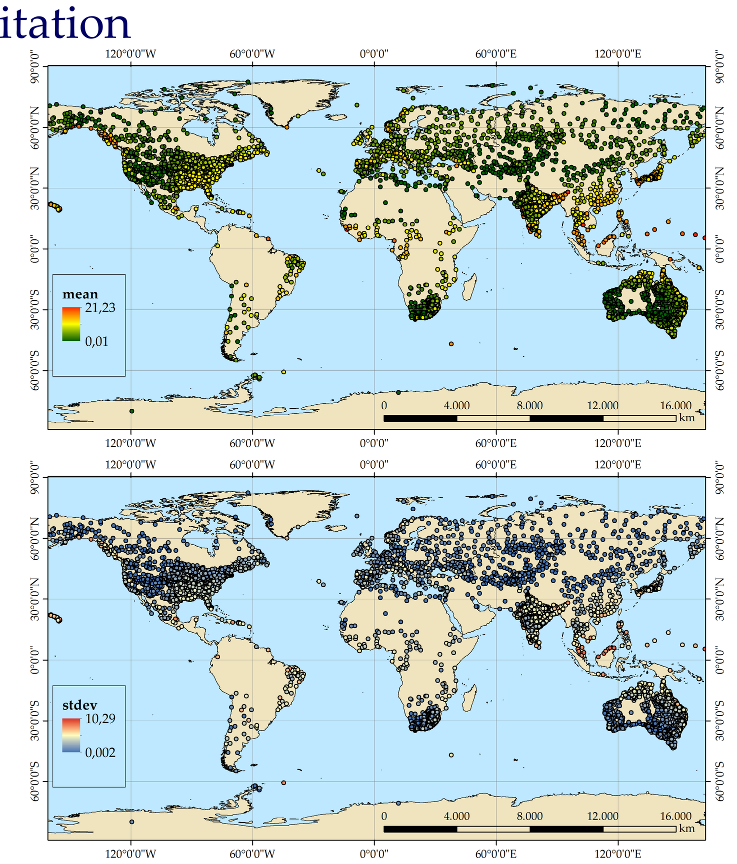

Map 2 & 3:Best stations (mean, stdev)

8. Estimation of the prediction intervals for a high credibility station

The station analyzed below, is the one with the higher quality and is located in the North - East Australia. It corresponds to the group A by Koppen of tropical climates with constant high temperatures for all 12 months of the year and that also have average temperatures of 18 °C (64.4 °F) or higher. The subdivision group is the Af (tropical rainforest climate) where all 12 months have an average precipitation of at least 60 mm (2.4 in). This climate is dominated by the doldrums low-pressure system all year long, so it has no natural seasons.

Specifically, from the analysis made, the probability dry for this station approaches 55% and with a mean value estimated as 9.64mm and standard deviation estimated as 26.59mm.

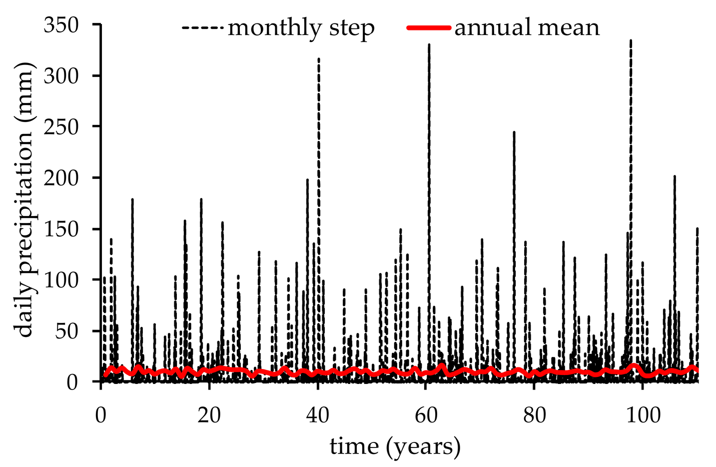

Figure 5: Precipitation timeseries recorded at the examined station.

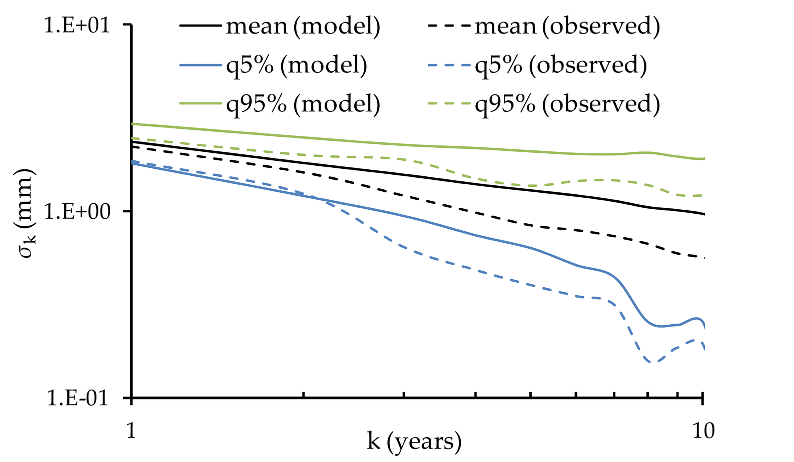

Figure 6: Climacograms for the selected station.

9. Estimation of the prediction interval for a high credibility station (cont.)

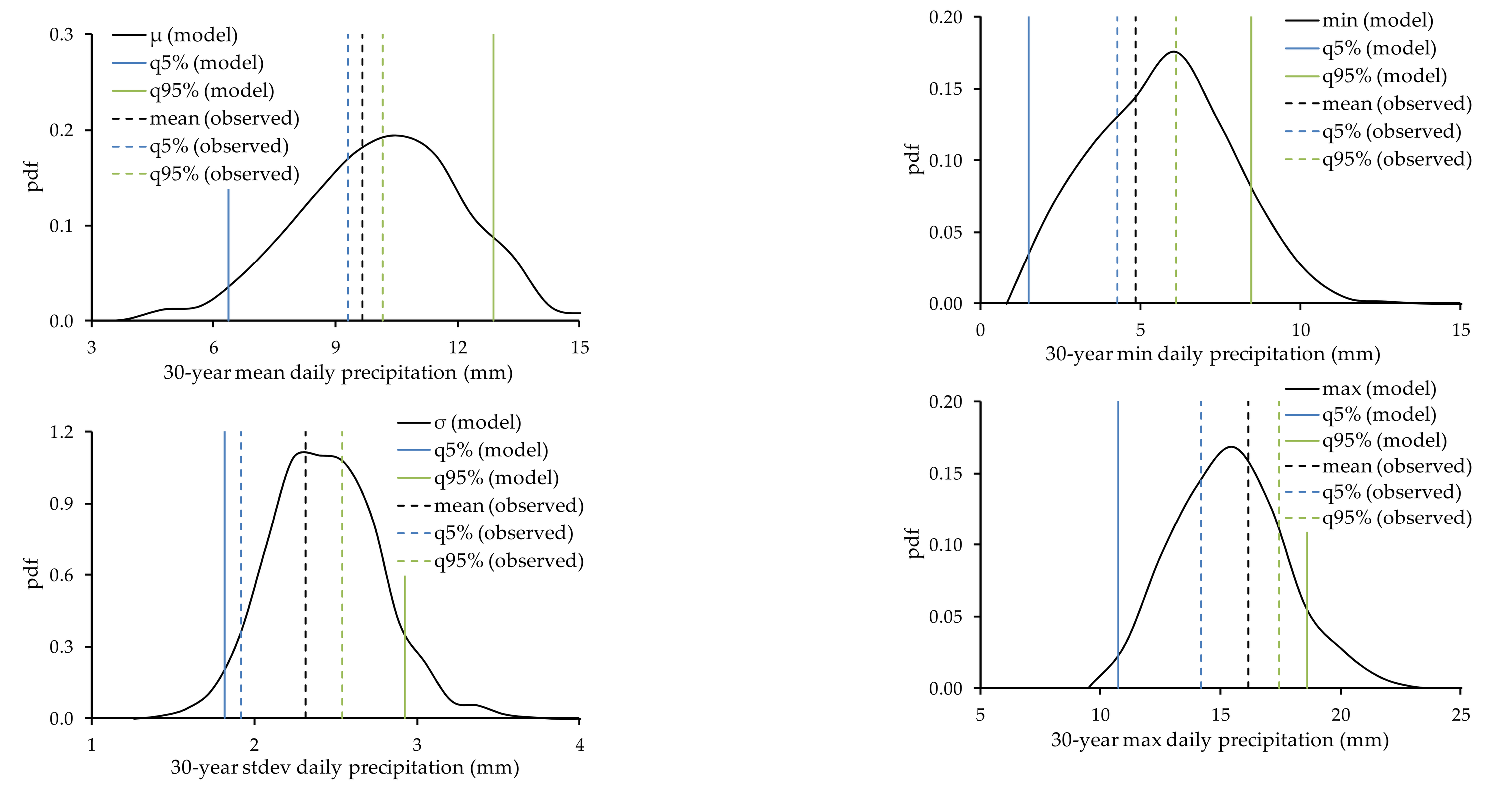

Figure 7: Estimation of prediction intervals for the examined station.

10. Hurst coefficient of annual mean precipitation

At this map, it can be noticed that along seaside areas the empirical Hurst is estimated as high as 0.75. This means that there might be a persistence behaviour on the precipitation near the sea. In addition, the empirical Hurst coefficient is estimated between 0.5 and 0.75 at areas located at the USA, Europe and Australia with numerous years of observations.

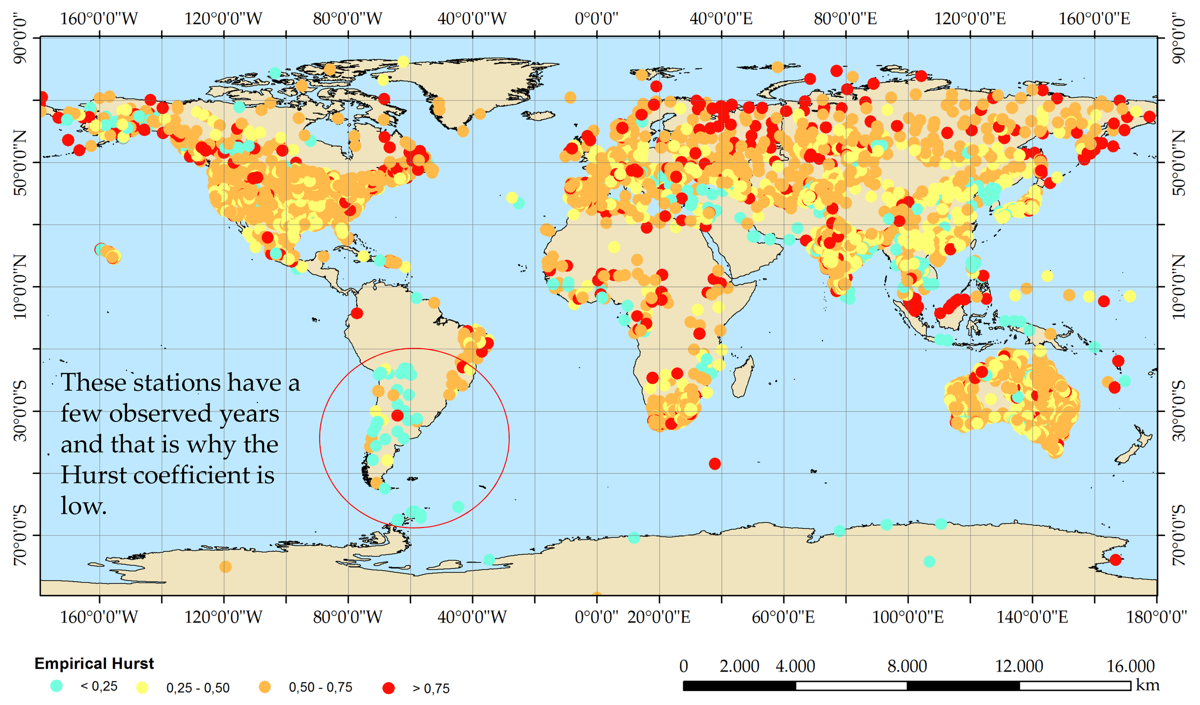

Map 5: Empirical Hurst coefficient.

11. Prediction Measure

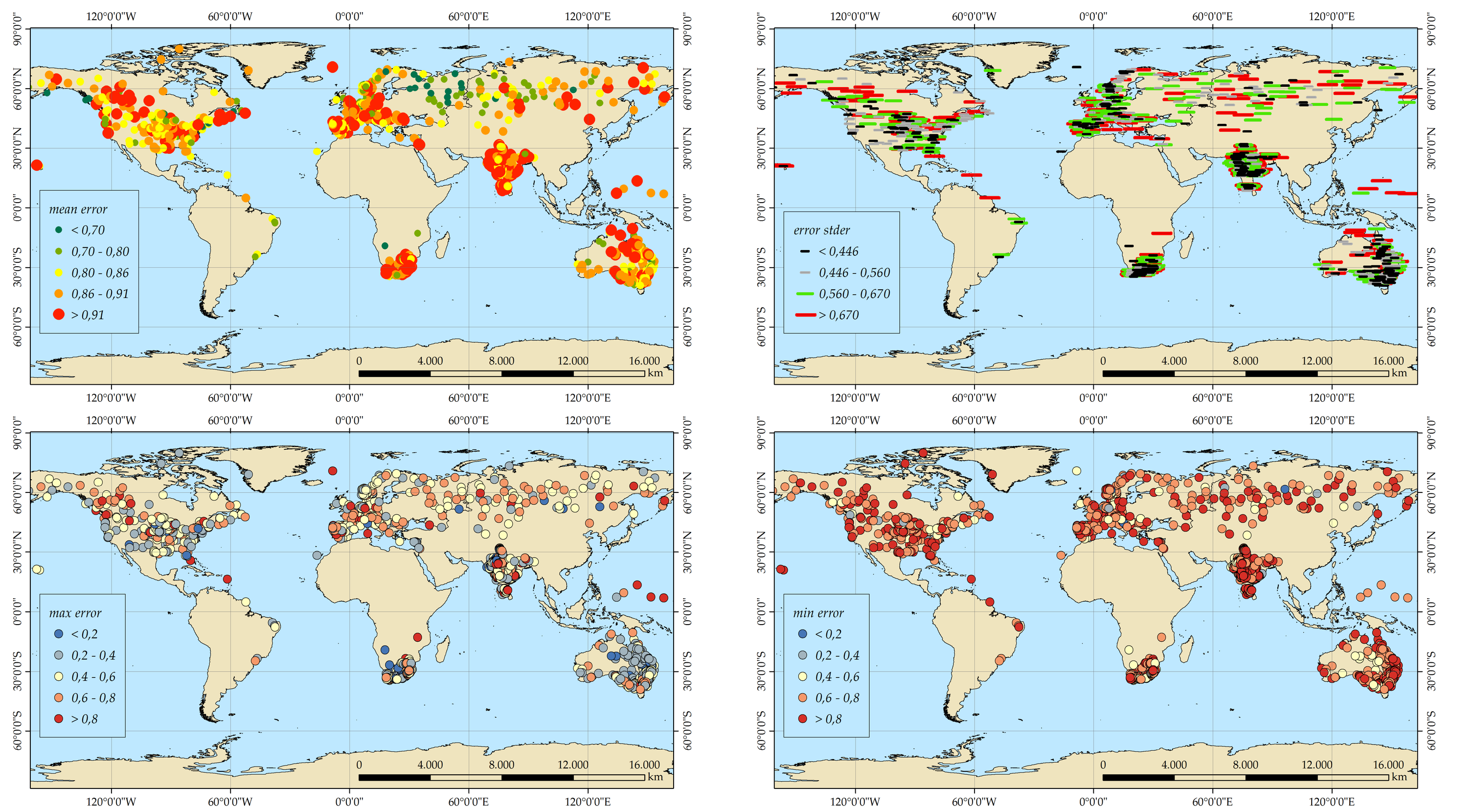

Map 6: Prediction Measure of mean, stdev, max and min values.

12. Conclusion

From the above analysis, it can be concluded that it is possible to describe the climatic variability of precipitation just by using three parameters (i.e., mean, standard deviation and Hurst coefficient).

- The distribution of our data, approximates the Gaussian distribution in the main body but not the tails.
- Via the method of the prediction error, we could predict the value of the 30-year mean for each station.
- The theoretical values of the Hurst coefficient were adequately estimated through the climacogram. These values are also classified by Koppen, but with not showing important differences and variations.
- The map of the spatial distribution of the Hurst coefficient around the globe, shows that the values ranged between 0.5-0.7 are all around Europe, USA and Australia. These values are estimated from stations that they have numerous precipitation measurements and therefore, these values are considered to be reliable.
- The stations located close to coastline, exhibit larger values of Hurst coefficient (over 0.75).
- Last but not least, it can be observed that the standard deviation increases along with the mean precipitation.

References

[1] Dore, Mohammed HI. "Climate change and changes in global precipitation patterns: what do we know?." Environment international 31.8, 1167-1181, (2005).
[2] G. G. Anagnostopoulos , D. Koutsoyiannis. "A comparison of local and aggregated climate model outputs with observed data." Hydrological Sciences Journal, (2006).
[3] D. Koutsoyiannis, The Hurst phenomenon and fractional Gaussian noise made easy, *Hydrological Sciences Journal, 47 (4), 573–595, 2002.*
[4] Dimitriadis, P., and D. Koutsoyiannis, Climacogram versus autocovariance and power spectrum in stochastic modelling for Markovian and Hurst–Kolmogorov processes, Stochastic Environmental Research & Risk Assessment, 29 (6), 1649–1669, doi:10.1007/s00477-015-1023-7, 2015.
[5] M. C. Peel, B. L. Finlayson, T. A. Mcmahon. "Updated world map of the Köppen-Geiger climate classification." Hydrology and Earth System Sciences Discussions, European Geosciences Union, (2007).